MINISTERIO DA CIÊNCIA E TECNOLOGIA
INSTITUTO DE PESQUISAS ESPACIAIS

PUBLICATION NO
INPE-4197-RPE/544

TITULO/TITLE

RADON CONCENTRATION INVERSIONS IN THE TROPOSPHERE

AUTORES/AUTHORSHIP

Enio Bueno Pereira
Marco Antonio Maringolo Lemes

RESUMO-NOTAS/ABSTRACT-NOTES

INSTITUTO DE PESQUISAS ESPACIAIS

AUTORIZAÇÃO PARA PUBLICAÇÃO
AUTHORIZATION FOR PUBLICATION

PALAVRAS CHAVES/KEY WORDS (AUTORES/AUTHORS)

TROPOSPHERE RADON
TRACE-GASES RADIOACTIVITY

AUTORIZADA POR/AUTHORIZED BY

Marco Antonio Raupp
Diretor Geral

AUTOR RESPONSÁVEL / RESPONSIBLE AUTHOR

E. B. Pereira

DISTRIBUIÇÃO/DISTRIBUTION

- [ ] INTERNA / INTERNAL
- [x] EXTERNA / EXTERNAL
- [ ] RESTRITA / RESTRICTED

REVISADA POR / REVISED BY

V.W.J.H. Kirchhoff

CDU/UDC

551.510.52

DATA/DATE

July, 1987

PUBLICAÇÃO Nº / PUBLICATION NO

INPE-4197-RPE/544

ORIGEM / ORIGIN

DGA

PROJETO / PROJECT

RADON

Nº DE PÁG. / NO OF PAGES

21

ULTIMA PÁG / LAST PAGE

20

VERSÃO / VERSION

Nº DE MAPAS / NO OF MAPS

TÍTULO/TITLE

RADON CONCENTRATION INVERSIONS IN THE TROPOSPHERE

AUTORES/AUTHORSHIP

Enio Bueno Pereira
Marco Antonio Maringolo Lemes

RESUMO - NOTAS / ABSTRACT - NOTES

Vertical concentrations of radon in the lower troposphere were obtained in Southern Brazil up to 7km high and have shown unexpected inverted profiles. The presence of low pressure center systems southwest to the flight path suggested that these inversions might have been originated by a vertical transport mechanism based on the large scale circulation of developing synoptic systems. A simple friction-driven circulation model was constructed and the transport equation was solved. The results show that upward motions of 2.5 $cm.s^{-1}$ can induce the observed inversion.

OBSERVAÇÕES / REMARKS

This work was partially supported by the "Fundo Nacional de Desenvolvimento Científico e Tecnológico" under contract FINEP-537/CT. This work is being submitted to Journal Geophysical Research.

RADON CONCENTRATION INVERSIONS IN THE TROPOSPHERE

by

Enio Bueno Pereira

Marco Antonio Maringolo Lemes

Instituto de Pesquisas Espaciais

C.P. 515, S.J.Campos, S.P. 12201 - Brasil

ABSTRACT

Vertical concentrations of radon in the lower troposphere were obtained in Southern Brazil up to 7km high and have shown unexpected inverted profiles. The presence of low pressure center systems southwest to the flight path suggested that these inversions might have been originated by a vertical transport mechanism based on the large scale circulation of developing synoptic systems. A simple friction-driven circulation model was constructed and the transport equation was solved. The results show that upward motions of 2.5 $cm.s^{-1}$ can induce the observed inversion.

INTRODUCTION

The potential of radon and its radioactive decay products as atmospheric tracers has not been fully explored yet. This is particularly true when dealing with studies of vertical mixing in the free troposphere, above the planetary boundary layer. Very recently, this issue came back to discussion in a paper by Liu et al. (1984) on the basis of a compilation of several vertical radon concentration profiles.

The solution of the diffusion equation for radon in the troposphere predicts an exponential concentration decrease with height over the continents, except for the first few hundred meters above the ground (see, for example, Reiter, 1978). This has been experimentally confirmed by several authors (Moore et al., 1977; Lambert et al., 1982).

Neverthless, some authors have observed that in some circunstances these vertical concentration profiles greatly deviate from this simple diffusion law or may even show an inverted profile. Wexler et al., (1956) first explained this in terms of radon transported by air masses coming from continental sources far upstream through oceanic paths. Later, Machta (1960), and Birot et al. (1970) supported Wexler's hypothesis with more experimental data.

Our data obtained from airplane flights in the Southern Hemisphere also show these inverted profiles and an interpretation based on large scale developing synoptic systems is proposed.

INSTRUMENTS AND METHODS

A novel design of a mobile radon-gas collector and measuring device was flown on a twin engine fixed wing aircraft (EMB-110-B1, Embraer-Brazil) over a coastal area in Southern Brazil, between the cities of São José dos Campos ($23^{o}18'S$, $45^{o}45'W$) and Lages ($27^{o}48'S$, $50^{o}20'W$), roughly 70 and 150km inland from the coastline, respectively (Figure 1). The flightwas made at two heights, 3km and 7km, during a single day in July, 1984. A second similar flight was made a month later.

The radon-gas collector and measuring device are shown schematically in Figure 2 and are described in detail in Pereira et al., (1985). Briefly, the air is filtered by a 0.45μm pore diameter membrane filter, after which the air enters a $0.042m^3$ precipitation chamber. The radon daughters produced inside this chamber (positive ions) are continuously precipitated through an electrostatic field onto a silicon alpha particle detector which is also the collecting electrode.

The estimated sensitivity of the system is very high, of the order of 0.6 $pCi.m^{-3}$ STP[1] of radon. This instrument permits a nearly continuous real time radon-gas measurement. Integration times can be adjusted from 5 minutes to several hours. The radon isotope to be measured can be chosen either by performing the spectral analysis of the detector output (circuit B in Figure 2) or by employing a delay line in the gas inlet system in order to eliminate the two short-lived radon isotopes (^{220}Rn, ^{219}Rn).

---

(1) 1 Ci = 3.7×10^{10} s^{-1}.

The air flow through the system was kept constant regardless of the airspeed and altitude of the airplane. This permitted an easy calculation of the real air flow through the system for each altitude.

EXPERIMENTAL RESULTS

The radon concentration profiles obtained with our radon-gas collector are shown in Figure 3, along with profiles obtained by several authors in different places. These other profiles were all obtained from the published literature by selecting only those profiles which showed strong deviations from the simple exponential diffusion law.

Although these profiles correspond to experiments performed at different times and places, thus hindering precise comparisons, there is at least one feature that is common in all of them: a relative minimum between 2 and 4 kilometers. This steep change of slope in the concentration profile as also shown in the compiled average performed by Liu et al. (1984) and attributed to summer induced vertical transport mechanisms.

Our data obtained during Southern Hemisphere winter also show such feature, leading to the conclusion that the vertical flux responsible for the inverted profile of radon is not a characteristic of the summer season only.

Some authors (Machta, 1960; Guedalia et al., 1972; and Whittlestone, 1985) have attributed the inversions to continental air masses that have performed a long trajectory over an ocean. Owing to the short transit time of such air masses at upper atmospheric

levels, and also to the negligible radon production above the oceans, the net effect should be an inversion in the vertical concentration profile.

Convection within a single cumulus cloud, as pointed out by some authors (Wilkenning, 1970; Liu et al. 1984), is an efficient vertical transport for radon in the 3 to 8 kilometers region of the troposphere. The ground air loaded with radon is drawn near the cloud top by the active updrafts. This vertical transport mechanism is discussed by Gidel (1983) for certain chemical tracers in the atmosphere.

The sea breeze circulation should also be considered as one of the possible mechanism to explain the inversions for data collected over coastal areas. However, this mechanism would, at best, place the relative minimum radon concentration at a level just below the return current of the sea breeze cell which is lower than the 3 kilometer minimum in Figure 3.

We suggest a large-scale developing synoptic system to account for the vertical transport of radon. These deep tropospheric systems have typical horizontal scales of 1000 kilometers and may extend up to the tropopause. Their associated vertical motions, however, are much smaller than those of an active cumulus cloud but, as will be theoretically shown in this paper, can provide the required vertical transport to explain the profile modifications as observed.

The prevailing synoptic situation on July 11, as given in Figure 1, shows a low pressure center located at 30^{0}S, 57^{0}W with 1012.6mb and its associated cold front extending northward. Another

system with its low off the Rio Grande do Sul coast had already passed the region, and the influences of its cold front, with a more zonal orientation, are still present.

Regions of ascending motions occur in the sector bounded by the two fronts, being more pronounced in their neighborhoods. The upper level circulation as inferred from a GOES satellite image for the same day shows a trough west to the flight path, which is conducive to rising motions in the area. The unavailability of conventional upper air data has made this analysis somewhat crude. Nevertheless the principal configurations of the synoptic scale circulation are present in the analysis sketched in Figure 1.

The second flight, on August 10, presented a similar synoptic situation (not shown), with a low pressure center located approximately at $25^{o}30'S$, $57^{o}30'W$.

THE SYNOPTIC CIRCULATION MODEL

A simplified model of a purely friction-driven circulation has been choosen in order to simulate the primary characteristics of a developing synoptic system. In this model, surface air converges towards the low pressure center and, by continuity, is forced to rise. Directly above the surface low, and just below the tropopause which acts as a constraint to vertical motions, the air diverges away from an upper level high. This circulation is an idealization of that associated with the developing of a surface low pressure system and its corresponding cold front.

The convective transport of radon in the troposphere can be described by the transport equation in cylindrical coordinates (Wilkening, 1970):

$$k_z \frac{\partial^2 r}{\partial r^2} + \frac{\partial n}{\partial r}\left\{\frac{k_z}{r} - \langle u_r \rangle\right\} + k_z \frac{\partial^2 n}{\partial z^2} - \langle u_z \rangle \frac{\partial n}{\partial z} - \lambda n + \langle q \rangle = 0 \qquad (1)$$

where

n = atomic concentration of radon (m^{-3});

k_z = vertical component of the eddy diffusivity ($m^2.s^{-1}$);

$\langle u_r \rangle$ = time averaged radial wind component ($m.s^{-1}$);

$\langle u_z \rangle$ = time averaged vertical wind component ($m.s^{-1}$);

λ = decay constant of ^{222}Rn (s^{-1});

$\langle q \rangle$ = time averaged radon production rate ($m^{-3}.s^{-1}$).

For the sake of simplicity, we will not consider the curvature of the Earth. The maximum vertical distance error introduced by this simplifying assumption is only 0.8%, for horizontal distances of the order of 10^6m.

The model used to reproduce the structure of the circulation of a deep pressure system assumes the balance of a baroclinic pressure gradient force, the Coriolis force, and friction. In this model, the frictional force is expressed in terms of the Guldberg-Mohr equation being proportional and of opposite sense to the velocity vector. This force balance in isobaric coordinates is given by

$$-fv = -\frac{\partial \phi}{\partial x} - \alpha u, \qquad (2)$$

$$fu = -\frac{\partial \phi}{\partial y} - \alpha v, \tag{3}$$

where (u, v) are the zonal and meridional wind components respectively, f the Coriolis parameter, and α the coefficient of proportionality. The prescribed perturbation geopotential, ϕ, is given by

$$\phi(x, y, p) = \phi_0 \cos\left[\frac{\pi p}{p_0}\right] \exp -(r/R)^2, \tag{4}$$

where ϕ_0 is a constant, p_0 is the uniform surface pressure taken as 1000mb. The constants were chosen to yield representative values for typical horizontal winds (Table 1).

Solving u and v in terms of ϕ and integrating the continuity equation with respect to the pressure p under the assumption that the isobaric vertical motion, w, vanishes at p = po, one arrives at:

$$\langle w(r,p)\rangle = -\int_{p_0}^{p}\left[\frac{\partial u}{\partial x} + \frac{\partial v}{\partial y}\right] dp' \tag{5}$$

The vertical motion, $\langle u_z \rangle$, in geometric heigh coordinate system is approximately given by:

$$\langle u_z \rangle \approx \frac{4\phi}{R^2}\,\frac{\alpha}{f^2+\alpha^2}\,\frac{R^2-r^2}{R^2}\exp -(r/R)^2\left[\frac{p_0}{\pi}\right]\sin\frac{\pi p}{p_0}\,(\rho g)^{-1}, \tag{6}$$

where ρ is the height dependent density, and g is the acceleration of gravity.

The solution of Equation (1) requires the radial component of the horizontal wind to be known. This component, as

well as the azimutal one, is easily determined from the Cartesian components, u and v are as given by Equation (2) and (3). They are:

$$\langle u_\theta \rangle = -\frac{2\phi}{R^2}\,\frac{f}{f^2+a^2}\; r \exp -(r/R)^2 \cos\frac{\pi p}{p_0}\,, \tag{7}$$

$$\langle u_r \rangle = \frac{2\phi}{R^2}\,\frac{a}{f^2+a^2}\; r \exp -(r/R)^2 \cos\frac{\pi p}{p_0}\,, \tag{8}$$

The finite difference equation corresponding to Equation (1) was obtained by calling $r = ih$ and $z = im$, for $i = 1, 2, 3, \ldots$, with h and m being the finite radial and vertical increments, respectively. Thus,

$$n_{i+1,j}\left\{\frac{k_z}{h^2}+\frac{1}{2h}\left[\frac{k_z}{ih}-\langle u_r\rangle\right]\right\} + n_{i-1,j}\left\{\frac{k_z}{h^2}-\frac{1}{2h}\left[\frac{k_z}{ih}-\langle u_r\rangle\right]\right\} +$$

$$+ n_{i,j}\left\{\frac{2k_z}{h^2}+\frac{2k_z}{m^2}+\lambda\right\} + n_{i,j+1}\left[\frac{k_z}{m^2}-\frac{\langle u_z\rangle}{2m}\right] + \tag{9}$$

$$+ n_{i,j-1}\left[\frac{k_z}{m^2}+\frac{\langle u_z\rangle}{2m}\right] = -\langle q\rangle .$$

The boundary conditions to be satisfied by Equation (9) are:

$n(z = 0)$ = n_0, the sea level global average radon concentration;

$n(z = z_\infty)$ = 0

$\partial n/\partial r]_{r=0} = \partial n/\partial r]_{r=r_\infty} = 0.$

The outermost boundary condition is applied at r_∞ = 1400km, where the circulation is sufficiently weak so to minimize effects of artificial boundaries on the interior solution.

For the same reason $z_\infty = 18km$, a level well above the upper branch of the confined tropospheric circulation.

The parameters of the model are listed in Table (1) based upon realistic data.

TABLE 1. Parameters of the Model

$k_z = 10m^2.s^{-1}$ (z)

$\lambda = 2.1 \times 10^{-6}\ s^{-1}$,

$n_0 = 10^6\ m^{-3}$,

$f = -7.29 \times 10-5\ s^{-1}$,

$R = 8 \times 10^5 m$,

po = 1000mb,

$\phi = 1000m^2.s^{-1}$ (primary circulation wind of $10m.s^{-1}$),

$\alpha = 0.25 \times 10^{-5}$ to 1.0×10^{-5}.

z The eddy diffusion coeficient is constant through the troposphere. In the tropopause it decreases exponentially to a value of $0.1m^2.s^{-1}$ at 18km.

DISCUSSIONS AND CONCLUSIONS

Figure 4a shows the simple exponential concentration law for radon, when the vertical transport is completely supressed. This computer run was used in addition to validade the numerical model.

To test the proposed mechanism for the concentration inversions, a series of model outputs is shown in Figure 4b through 4d, focusing on the response of the model to vertical motions of different intensities. This was acomplished by changing the coefficient, α, in the governing equations of the large scale circulation model. As can be seen in Equation 8, for values of $\alpha < f$, the effect of increasing α is to increase the divergent component of the large-scale wind, $\langle u_r \rangle$, as well as the divergence field itself. In return, this causes the vertical component, $\langle u_z \rangle$, to change in order to satisfy the constraint imposed by the continuity equation.

Values of k_z within the range of 5 to 15$m^2.s^{-1}$, which are very likely to occur in the troposphere, do not appreciably change the concentration inversion characteristic found for the model. Therefore, we adopted for k_z a values of 10$m^2.s^{-1}$ following Hunten (1975). The sharp transition of k_z in the tropopause, however, has been prudently smoothed in order to prevent problems with the finite-difference method.

The evolution of the isoconcentration lines shows the effects of imposing an initial vertical wind[3] ($\langle u_z \rangle_{max} = 1.2 cm.s^{-1}$) in Figure 4b. As the updrafts current increase, more radon is swept from the ground towards the low pressure center where it is raised to upper levels. The continuity equation guarantees the return of this radon somewhere in the return current which extends up to the infinite.

---

(3) We shall define here the maximum vertical wind $\langle u_z \rangle_{max}$, which occurs at $r = 0$ and $z = H/2$, where H is the height of the circulation cell.

Figure 4c shows the onset of an inverted concentration profile for $\langle u_z \rangle_{max} = 2.5 cm.s^{-1}$. At larger updraft velocities in the model the inversions are even more pronounced, as expected (Figure 4d).

As one goes farther away from the low pressure center the upper level radon decays to background concentrations so that the inversions vanish and one ends up with the normal exponential decreasing concentration law.

A closed cycle by itself, however, does not provide the inversions of radon. An hypothetical stable and inert trace-gas would only be mixed up and homogenized by such a process. It is the combination of an adequate vertical transport, $\langle u_z \rangle$, and the radioactive decay constant of radon, λ that assures the concentration inversions.

One should expect a transit time of a parcel of ground air loaded with radon that reaches the upper level layers of the troposphere, of the order of a few radon half-lives at most so to produce a measurable inverted profile. In fact, for a radon half-life transit time (3.82 days), one finds a corresponding updraft speed $\langle u_z \rangle_{max}$ of $3.03 cm.s^{-1}$, which is of the right order of magnitude.

The results of both the July 11 and August 10 flights emphasize the need of a controlled experiment with good support of meteorological data in order to shed more light to this problem. Nevertheless, our preliminary study based on available data of the prevailing synoptic situation, and the results of our simplified numerical model, indicate that the large-scale motions of a synoptic

developing system could be responsible for an inversion in the radon vertical concentration profile.

REFERENCES

BIROT, A.; ADROUGUER, B. and FONTAN, J., Vertical distribution of radon 222 in the atmosphere and its use for study of exchange in the lower troposphere, *Journal of Geophysical Research*, 75(12): 2373-2393, 1970.

GIDEL, L.T., Cumulus cloud transport of transient tracers, *Journal of Geophysical Research*, 88(C11):6587-6599, 1983.

GUEDALIA, D.; LOPEZ, A.; FONTAN, J. and BIROT, A., Aircraft measurements of radon 222 Aitken nuclei and small ions up to 6km, *Journal of Applied Meteorology*, 11:357-365, 1972.

HUNTEN, D.M., Vertical transport in atmosphere, in: *Atmospheres of Earth and Planets*, Edited by B.M. McConnart, pp. 59-72, Dordrecht, Holland, 1975.

LAMBERT, G.; POLIAN, G.; SANAK, J.; ARDOUIN, B.; BUISSON, A.; JEGOU, A.; et LE ROULLEY, J.C., Cycle du radon et de ses descendants: application à l'étude des échanges troposphère-stratosphère, *Ann. Geophys.*, 32(4):497-531, 1982.

LARSON, R.E., Radon profiles over Kilauea, the Hawaiian islands and Yukon valley snow cover, *Pure and Applied Geophysics*, 112:204-208, 19874.

LIU, S.C.; McAFFE, J.R. and CICERONE, R.J., Radon-222 and tropospheric vertical transport, *Journal of Geophysical Research*, 89(05):7291-9297, 1984.

MACHTA, L., Inverted concentration profiles from a ground source, *Journal of Meteorology*, 18:112-113, 1960.

MOORE, H.E.; POET, S.E. and MARTEL, E.A., ^{222}Rn, ^{210}Pb, ^{210}Bi, and ^{210}Po profiles and aerosol residence times versus altitude, *Journal of Geophysical Research*, 78(30):7065-7075, 1973.

MOORE, H.E.; POET, S.E. and MARTELL, E.A., Vertical profiles of ^{222}Rn and its long-lived daughters over the eastern Pacific, *Environment Science and Technology*, 11(13):1207-1210, 1977.

PEREIRA, E.B.; NORDEMANN, D.J.R.; TAKASHIMA, A.M.; DUTRA, L.S.V.; MANTELLI NETO, S.L., Um sistema para monitoração do radônio e seus produtos de decaimento na atmosfera, *Revista Brasileira de Geofísica*, 2:59-64, 1985.

REITER, E.R. (Edt.), *Atmospheric transport process - part 4: radioactive tracers*, pp. 28, available from NTIS - U.S. Department of Commerce, Springfield, Virginia 22161- 1978.

WEXLER, H.; MACHIA, L.; POCK, D.H. and WHITE, F.D., Atomic energy and meteorology, *Proc. of the International Conference on the Peaceful Uses of Atomic Energy*, Geneva, vol. 13, pp. 333-344, 1956.

WHITTLESTONE, S., Radon monitoring as an aid to the interpretation of atmospheric monitoring, *Journal of Atmospheric Chemistry*, 3: 187-201, 1985.

WILKENING, M.H., Radon-222 concentration in the convective patterns of a mountain environment, *Journal of Geophysical Research*, 75(9):1733-1740, 1970.

FIGURE CAPTIONS

FIGURE 1 - Schematic analysis of the synoptic situation in the area of the July 11 flight, depicting the surface fronts and the upper level circulation as inferred from a GOES satellite image. The flight path is also shown in this Figure.

FIGURE 2 - Radon-gas collector and measuring device employed in this experiment. The single-channel analyser is set to accept only energies between 6.00 MeV and 7.68 MeV of ^{218} Po and ^{214} Po, respectively. This procedure greatly increases the signal-to-noise ratio of the data by preventing electronic noise, low energy alphas and betas from entering the counting system.

FIGURE 3 - Several inverted radon concentration profiles compiled from the published literature.

□ Wexler et al. (1956); ◇Guedalia et al. (1972); o Moore et al. (1973); + Larson (1974); ● Our data 07/11/84; ▲ our data 08/10/84. Error bars are indicated, and total sampled volume ranged from 834 to 1896 litres.

FIGURE 4 - Results of the model calculation showing the onset of the concentration inversion of radon. The lines are the isoconcentration of ^{222} Rn (m^{-3}) starting from a ground concentration of 10^6 m^{-3} (114 $pCi.m^{-3}$). A - is the representation of the radon vertical profile in the absence of the transport term $\langle u_z \rangle$ in Equation (1). B - is for $\langle u_z \rangle_{max} = 0.012 m.s^{-1}$. C - is for $\langle u_z \rangle_{max} = 0.025 m.s^{-1}$. D - is for $\langle u_z \rangle_{max} = 0.05 m.s^{-1}$.

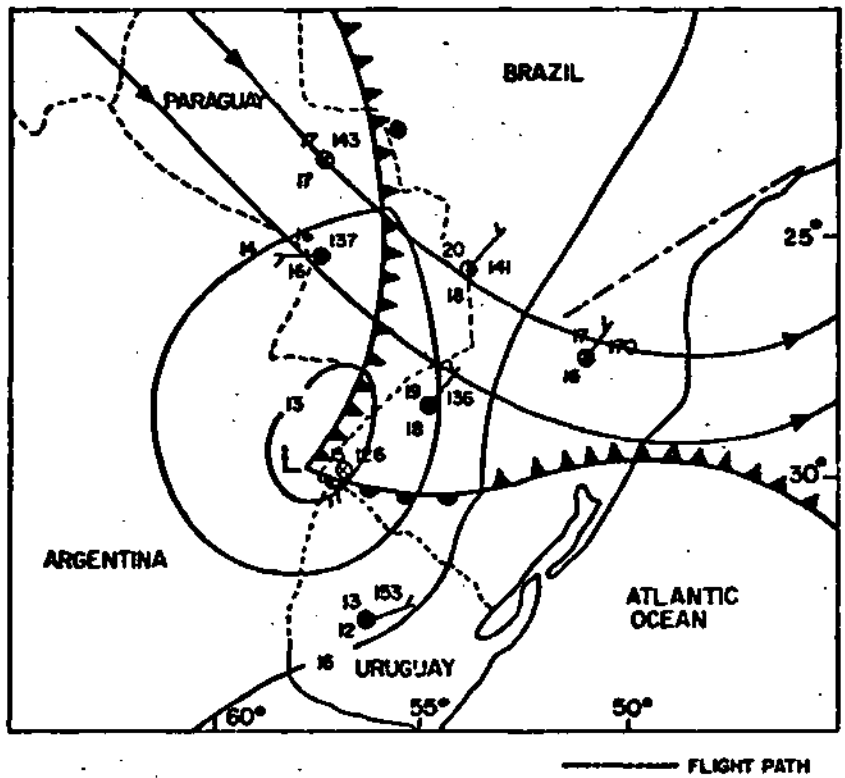

FIGURE 1 - Schematic analysis of the synoptic situation in the area of the July 11 flight, depicting the surface fronts and the upper level circulation as inferred from a GOES satellite image. The flight path is also shown in this Figure.

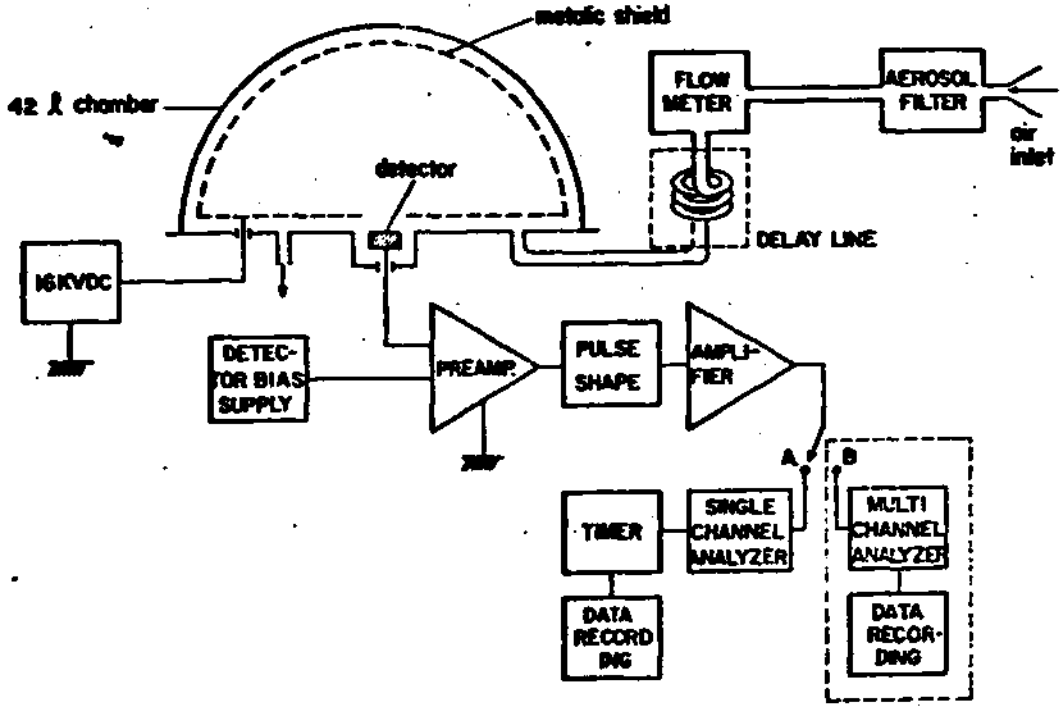

FIGURE 2 - Radon-gas collector and measuring device employed in this experiment. The single-channel analyser is set to accept only energies between 6.00 MeV and 7.68 MeV of ^{218}Po and ^{214}Po, respectively. This procedure greatly increases the signal-to-noise ratio of the data by preventing electronic noise, low energy alphas and betas from entering the counting system.

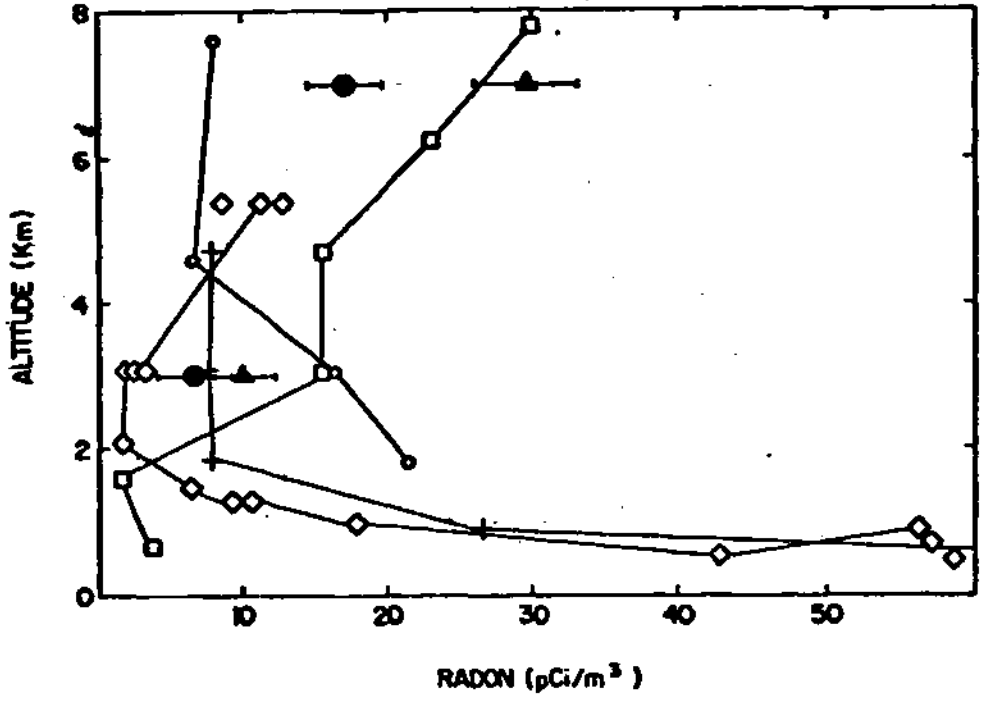

FIGURE 3 - Several inverted radon concentration profiles compiled from the published literature.

□ Wexler et al. (1956); ◇ Guedalia et al. (1972); o Moore et al. (1973); + Larson (1974); ● Our data 07/11/84; / our data 08/10/84. Error bars are indicated, and total sampled volume ranged from 834 to 1336 litres.

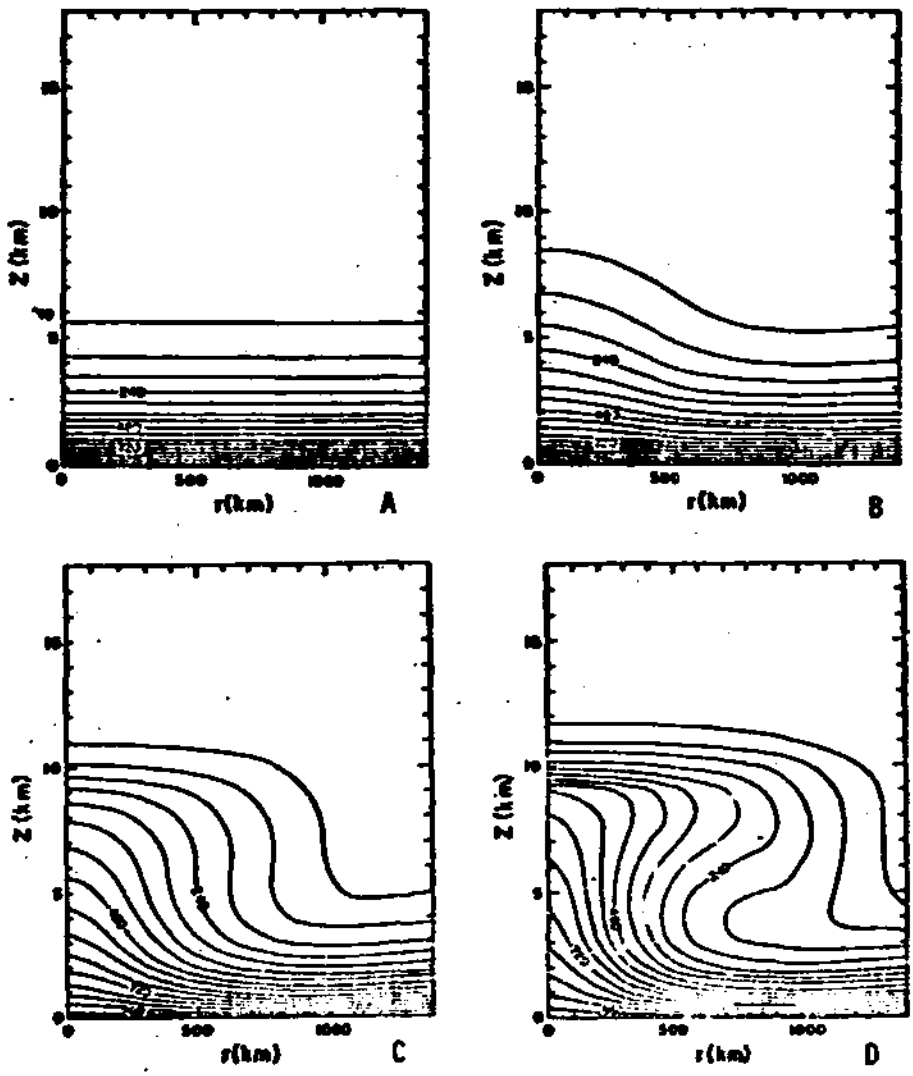

FIGURE 4 - Results of the model calculation showing the onset of the concentration inversion of radon. The lines are the isoconcentration of ^{222} Rn (m^{-3}) starting from a ground concentration of 10^{6} m^{-3} (114 $pCi.m^{-3}$). A - is the representation of the radon vertical profile in the absence of the transport term $\langle u_z \rangle$ in Equation (1). B - is for $\langle u_z \rangle_{max}$=0.012m.$s^{-1}$. C - is for $\langle u_z \rangle_{max}$=0.025m.$s^{-1}$. D - is for $\langle u_z \rangle_{max}$=0.05m.$s^{-1}$.